4th GRACM Congress on Computational Mechanics
GRACM 2002
Patra, 27-29 June, 2002

A SEARCH ON THE INSTABILITY OF FRAME STRUCTURES TESTED TO BUCKLING UNDER SIDE SWAY

Dr Philotheos G. Lokkas

Professor of TEI of Larissa
Laboratory of Strength of Materials
TEI of Larissa, 411 10 Larissa, Greece
e-mail: p.lokkas@teilar.gr, web page: http://www.teilar.gr/~p.lokkas

Keywords: Sway, Non-sway, Frame, Buckling

Abstract: *The importance on collapse of rigid jointed frames when sway and non-sway critical modes exhibit simultaneous or nearly simultaneous critical loads is presented in this project. Current design methodologies for framed structures having the possibility of side sway in their plane, assume failure occurs either as a result of column buckling, where the column, considered as a member, is loaded in compression or a combined action of it with bending, or as a result of frame instability. If the buckling load of column is significantly higher than that required to initiate instability of frame (or vice versa), then much of the construction load carrying capacity remains unutilized. An efficient design, would therefore aim to produce simultaneity of instability in both the column as a member and the frame as a whole construction, something for which an engineer normally pays considerable attention by selecting the column section with respect to the surrounding frame stiffness. The project covers the results of an experimental study made to evaluate the load carrying capacity of a frame construction in the presence of imperfections, where, the critical loads of instability (member – frame) are close to each other.*

1 INTRODUCTION

1.1 The Problem

Current design practice for framed structures encourages designers to detail components to fail simultaneously in possibly a variety of different modes. In buckling design procedures for such structures, having the possibility of side sway, the designers are implicitly encouraged to attain a state, where for any column, considered as a part of a frame, two buckling modes, sway and non-sway occur simultaneously.

If we think of an axially loaded column, which is a part of a non-braced frame, i.e. a frame having the possibility of side-sway, then two different kinds of instability have to be considered:

a) A member instability for the column, which is the classic case of buckling, known as non-sway buckling mode and

b) A frame instability, arising from the property of the frame to be non-braced, known as sway mode.

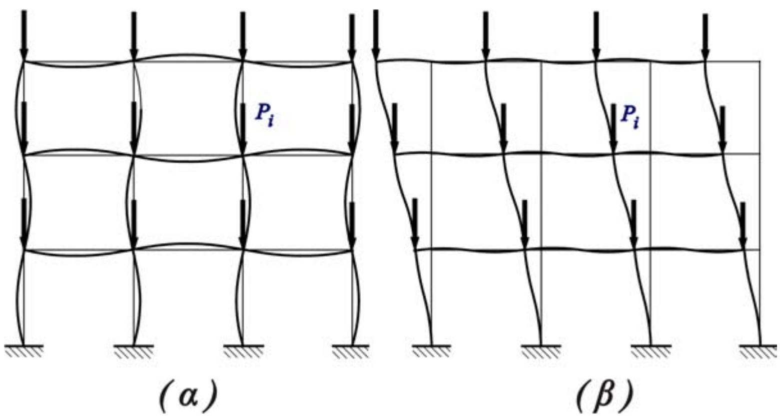

Figure 1: Instability of Frames

If the surrounding the column stiffness of the frame results in the first two critical loads having totally different values, each mode can be considered separately and this case is normally covered by the current design practice.

What happens however, when the frame stiffness, combined with the stiffness of the column, results in close values of the first two critical loads? This situation of course is not a virtual one. Designers, even for a single column in buckling, are encouraged to reach this situation – in order to optimize the use of material – by changing the cross-section properties and lateral restraints. Moreover, what is the system's response going to be in the presence of imperfections in both modes? These questions are not adequately covered by the current design practice and highlight the significance of the problem.

The project presents an experimental procedure, which, taking into account the stiffness of the surrounding the column frame along with the effects of imperfections, leads to the load carrying capacity of the column. It extends past treatment of the elastic – plastic buckling in a single mode to circumstances where more than one mode contributes to the non-linear elastic behavior and consequently elastic-plastic failure [1], without developing theoretical concepts and equations.

1.2 Aims

This project targets to experimentally confirm the theoretical predictions coming from reference [2] and aims to present an experimental program with a parametric study on the load carrying capacity of an intermediate column which is a part of a non braced frame, i.e. a frame that has the possibility of side sway on its plane.

The experimental program has been designed to:

a. Provide a force controlled test rig which allows independent control of vertical and horizontal load levels required to cover a wide parametric range

b. Allow an extensive test program on different frame geometries to assess the validity of the theoretical model developed for both sway and non-sway buckling modes.

1.3 Failure Criterion

In order to determine the buckling strength of a column, it is necessary to define a failure criterion at which the column will be considered to have failed. For this reason the two limited cases given below are adopted.

First Yield formation, where the column is considered to have failed if the stress at some point in a cross section reaches the yield value. The load that causes the initiation of yielding is a lower bound to the collapse load of the column.

First hinge formation, where the column is deemed to have failed if the stress in a cross section has reached the yield value everywhere. The load that causes a plastic hinge to form, is an upper bound to the collapse load of column.

2 NOTATION

P_c Euler critical load.
P_{cS} Sway critical load.
P_{cN} Non-sway critical load.
P_b Buckling load.
P_y Squash load in the absence of bending moment.
P_{fy} First yield load.
P_{fp} First hinge load.
$L_{1,3}$ Length of columns.
$b_{1,3}$ Breadth of columns' cross section.
L_2 Length of beams.
b_2 Breadth of beam's cross section.
d Depth of beams or columns cross section.
$I_{1,3}$ Cross section's moment of inertia of columns with respect to the centroid axis.
I_2 Cross section's moment of inertia of beams with respect to the centroid axis.
ξ_S Sway total equivalent imperfection.
ξ_N Non-sway total equivalent imperfection.
ρ_s Sway imperfection parameter[2].
ρ_n Non-sway imperfection parameter[2].

3 THE TEST ENVIRONMENT

The frame shown in figure 2 consists of three columns and four beams. The beams have the same length and cross-section. The columns have the same length, but the central column may have a cross-section different from the outer two. In other words the frame geometry presents a symmetry with respect to the central column.

The frame is pin-supported on the bottom end of the central column while there are roller supports on the left and right bottom ends.

To connect the beams and columns to each other, so that the whole frame presents a monolithic behavior, special end blocks had been constructed. In this way we did not only avoid having welded connections – thus keeping the cost of replacement low – but more important, we eliminated any uncertain characteristics arising from the weld heat affected zone. Of course these connectors introduced complications in the calculations for the theoretical behavior of the frame.

On the top left of the frame a horizontal force could be applied through weights to introduce controlled non-proportional sway imperfections. On the other hand, putting loads on say, the top left and bottom right beams, we could similarly introduce on the central column non-proportional out of straightness non-sway imperfections.

In order to maintain the verticality of the axial load on the central column, a gantry was used, connecting the top of the central column with a wheel nut of a trolley mechanism. The trolley could move horizontally – following any top horizontal displacement – through a smaller wheel nut.

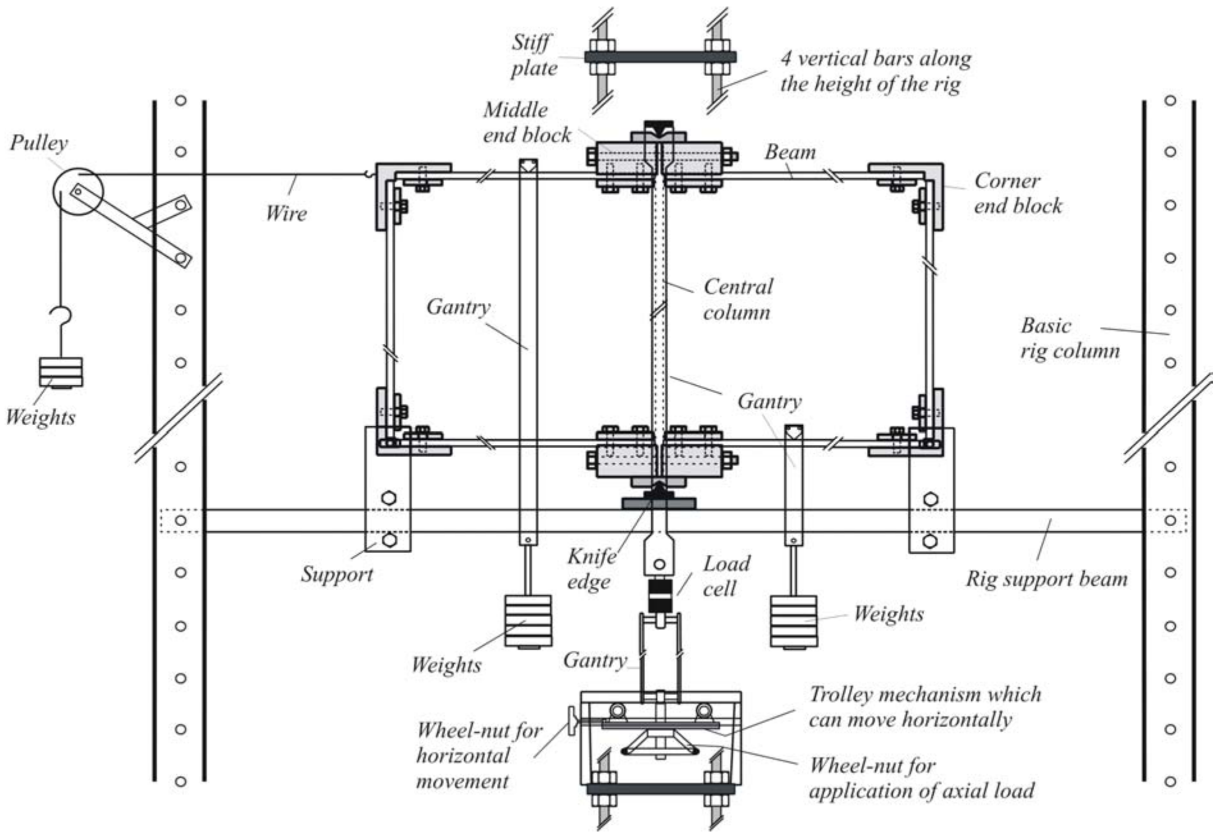

Figure 2: Overall arrangement of test – rig

The response was monitored by taking readings of the axial load, along with the top horizontal deflection of the frame and the deflection on the mid height of the central column.

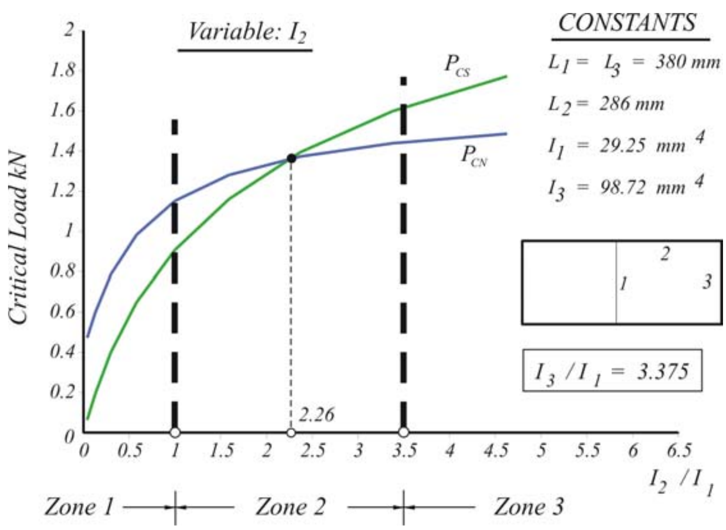

Figure 3: Typical parametric study for test models design.

In order to cover a large range of imperfection sensitivities, the frame geometries were intended to give non-sway over sway critical load ratios between 0.8 and 1.2. This was achieved by varying the beam lengths L_2 relative to those of the columns L_1=L_3, and selecting appropriate second moments of area of the beams as well as of the outer columns, relative to that of the central column.

Using three different beam stiffnesses, the interactive behavior was classified in three zones. In zone 1, shown in Figure 3, the sway critical load was less than the corresponding non-sway; in zone 3 the situation was reversed. Over zone 2, the most interesting, the sway and non-sway critical loads were close to each other.

The three classes of model frame chosen to cover the behavior of zone 2 are presented in table 1. The table summarizes the geometries, i.e. lengths and cross section sizes, along with theoretical predictions of the first two critical loads, material properties and the ratio of the sway over the non-sway critical loads for each frame.

Frame Class	**Model**	**L_1=L_3 mm**	**L_2 mm**	**b_1 mm**	**b_2 mm**	**b_3 mm**	**d mm**	P_{cS} **kN**	P_{cN} **kN**	P_y **kN**	P_{cS} / P_{cN}
$\frac{P_{cS}}{P_{cN}} \leq 1$	1	280	300	6	5	5	13	8.04	12.19	26.44	0.659
	2	270	350	5	5	5	13	6.53	8.66	22.45	0.754
	3	330	300	5	6	5	13	6.24	7.14	22.45	0.875
$\frac{P_{cS}}{P_{cN}} \approx 1$	4	340	314	5	6	6	13	6.75	6.75	22.45	1.000
	5	260	300	5	6	6	13	11.13	11.13	22.45	1.000
$\frac{P_{cS}}{P_{cN}} \geq 1$	6	210	250	3	5	3	13	5.20	4.46	13.85	1.170
	7	235	400	3	5	5	13	4.63	3.41	13.85	1.357
	8	235	370	3	5	5	13	4.89	3.45	13.85	1.416

Table 1 Geometric and critical buckling load properties

In setting-up the frame for testing, a lot of care was taken to ensure the frame was aligned in a vertical plane as a continuous frame. A very useful tool was the trolley mechanism, which allowed the axial load to always have a vertical alignment. Once the frame was assembled, the desired levels of the sway and non-sway imperfections were applied through the appropriate horizontal and local beam loads.

For each test sufficient loading and unloading cycles in the elastic range were undertaken. On the basis of lateral displacements recorded over the top and the middle height of the central column along with the corresponding axial loads, it was possible to apply a typical procedure to obtain the Southwell Plots for both the sway and the non-sway buckling modes. This procedure allowed accurate experimental interpretation of both the total equivalent imperfections and the classical critical loads of both the sway and non-sway modes.

Typical interpretations are shown in figure 4.

Once these interpretations were derived, loading was continued to determine the elastic-plastic failure loads.

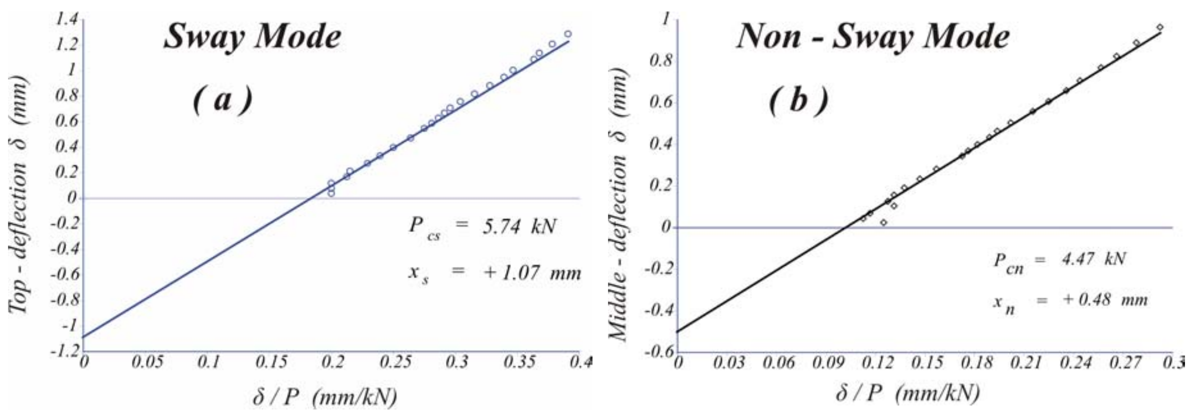

Figure 4: Interpretation of elastic test results using Southwell plot to find imperfections ξ_s , ξ_n along with critical loads P_{cS}, P_{cN}.

Despite the care taking to build the frame through the joint blocks, there remained some uncertainties. Theoretical critical loads differed from those obtained experimentally through Southwell approach. For model 6, for instance, shown in table 1, the theoretical sway critical load were 5.20 kN. However, due to inevitable but uncertain effects of friction, the experimentally obtained sway critical load was 5.74 kN.

The same did not apply with the non-sway mode, where, the two critical loads were nearly the same.

The results of all the sway and non-sway mode critical loads are summarized in the graphs of Figure 5, correlating the experimentally determined elastic critical loads against those predicted theoretically.

It is evident that scatter of the sway critical loads is greater than that exhibited by the non-sway. In most cases the scatter was within the 10% band.

When reliable results were obtained in the elastic range to interpret the total imperfections and the elastic critical loads, the test was repeated and the loading was increased to produce failure. Failures in the form of a maximum load, occurred fairly soon after the formation of first plasticity. Due to the nature of loading, which was displacement controlled, it was possible to observe equilibrium states beyond the maximum buckling load.

However, once a maximum load had been recorded along with small plastic deformations, the frame was unloaded.

Then the frame was retested with these additional permanent deformations, to find the new total imperfections and critical loads and subsequently a new maximum buckling load. Normally this procedure was repeated three times for each test frame.

4 TEST RESULTS

The experimental observations along with the theoretical predictions for a set of elastic-plastic tests on the 8 models used are summarized in table 2. It is clear that the load for the first yield P_{fy} represents as expected, a lower bound of the experimentally recorded buckling collapse load P_b. This lower bound represents the fairly considerable load reserve between the formation of first material failure and the number of fully formed plastic hinges for the total collapse.

Mo-del	Experimental Results					Theoretical Results				Comparisons	
	P_{cS} kN	P_{cN} kN	ξ_S mm	ξ_N mm	P_b kN	ρ_s	ρ_n	P_{fy} kN	P_{fp} kN	P_{fy}/P_b	P_{fp}/P_b
1	8.58	11.47	1.05	1.05	8.20	1.02	0.83	7.09	7.67	0.86	0.94
2	6.92	8.42	0.75	0.70	6.70	0.75	0.72	5.98	6.31	0.89	0.94
3	7.03	7.54	1.35	0.12	6.5	0.82	0.14	5.66	5.94	0.87	0.91
4	7.44	7.32	1.60	0.86	6.02	0.63	1.01	4.84	5.60	0.80	0.93
5	11.17	11.33	1.05	0.75	8.70	0.47	0.87	7.95	9.34	0.91	1.07
6	5.40	4.67	0.67	0.40	4.20	-0.09	0.80	3.44	3.86	0.82	0.92
7	4.20	3.76	0.80	0.05	3.80	-0.40	0.10	2.83	3.07	0.74	0.81
8	4.13	3.49	0.85	0.85	3.00	-0.58	1.68	2.70	3.00	0.90	1.00

Table 2: Comparisons between experimental observations and theoretical predictions for elastic-plastic buckling.

A somehow better way for predicting collapse is the load corresponding to the first plastic hinge P_{fp}. While this can not be guaranteed to produce a lower bound to collapse, it is evident that, for the majority of tests, it does provide close estimates of collapse. In general the load for the first hinge gives a more reliable prediction for the maximum buckling load.

5 CORRELATION OF TEST RESULTS

Figure 5 summarizes the results for all 28 tests on the 8 model geometries. Both the experimental buckling load P_b^{ex} and the theoretical predictions are normalized with respect to the lowest of the elastic critical loads, P_c.

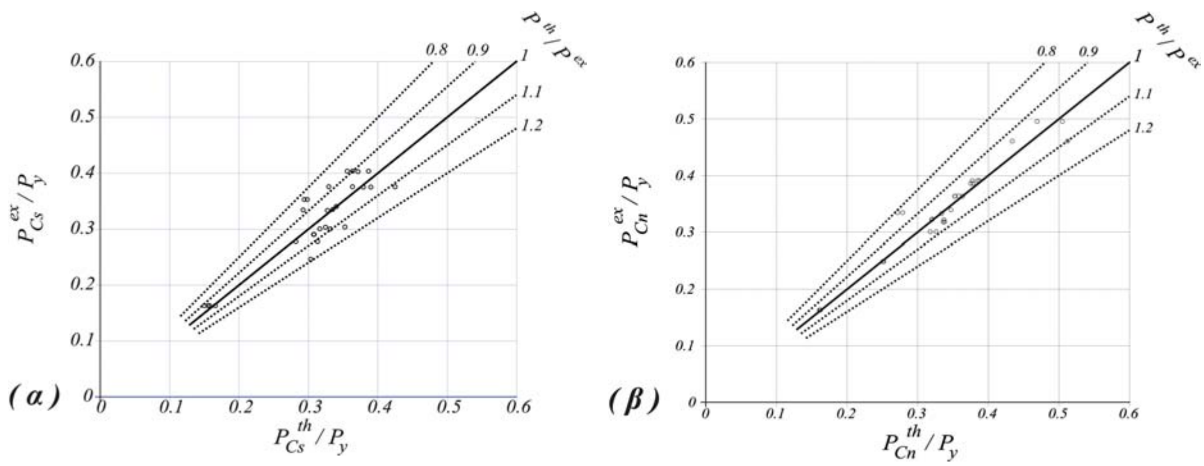

Figure 5: Correlations of the experimentally obtained critical loads and theoretical predictions for (α) sway and (β) non-sway critical loads.

These results confirm the findings shown in the comparisons between experiments and theory; first yield generally represents a reasonably reliable lower bound of collapse, with the scatter generally in the 0 to 20% scatter band.

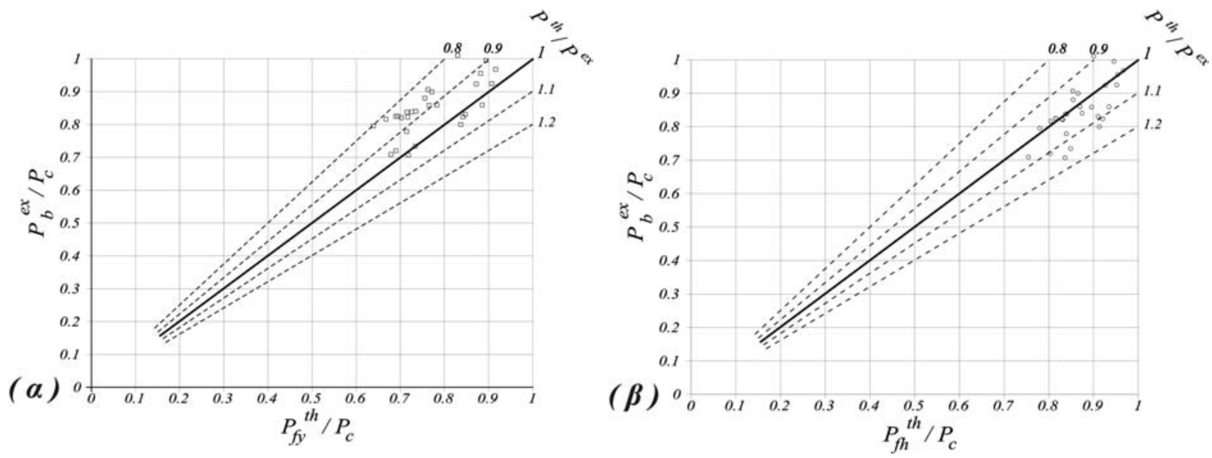

Figure 6: Correlation of the experimentally obtained maximum buckling load P_b^{ex} against (α) the theoretical prediction of the first yield load P_{fy}^{th} and (β) the load for first plastic hinge P_{fh}^{th}.

In figure 6, the results for both the first yield and the first full plasticity are similarly summarized. Here the scatter is more evenly distributed over the ±10% scatter bands and we cannot say that either an upper or lower bound can be provided.

In general, comparing the experimental buckling loads with the theoretical predictions, it is confirmed that theory and experiments are in a close coincidence.

First yield generally represents a reasonably reliable lower bound of collapse.

6 CONCLUSIONS

It was found that to provide sensible predictions of collapse, the effects of both the sway and the non-sway imperfections were required.

To base design on one of these imperfections could seriously affect the reliability of theoretical estimates of buckling.

If the effects of the sway and non-sway imperfections are to be adequately incorporated into future design it is suggested that a theoretical model along the lines of that described in reference [4] will be required.

7 REFERENCES

[1] Lokkas, P. (1996): ‘A consistent approach to the buckling design analysis of rigid jointed steel-frames subject to sidesway’, *PhD thesis*, University College London.
[2] Lokkas, P. (2002): ‘A rational approach on the study of a uniaxial buckling model’, to be presented at the *4th GRACM* Congress on Computational Mechanics 27-29 June.
[3] Lokkas, P. (2002): ‘A rational approach on the study of a biaxial buckling model’, to be presented at the *4th GRACM* Congress on Computational Mechanics 27-29 June.
[4] Lokkas, P. and Croll, J.G.A. (2000): ‘Theory of Combined Sway and Non sway Frames Buckling’, *ASCE*, Journal of Engineering Mechanics, Vol. 126, No. 1, pp. 84-92.